

# Relaxation of Segmental Orientation and Chain Extension in Polycarbonate Studied by Infrared Dichroism and Shrinkage

L. Lundberg, B. Stenberg, and J.-F. Jansson\*

Department of Polymer Technology, Royal Institute of Technology,  
S-100 44 Stockholm, Sweden

Received February 10, 1994; Revised Manuscript Received June 11, 1996<sup>®</sup>

**ABSTRACT:** The relaxation of the segmental orientation and the chain extension in polycarbonate have been studied by infrared dichroism and heat shrinkage after a step strain deformation to a draw ratio of  $\lambda = 1.75$ . This makes it possible to distinguish between local relaxation mechanisms (Rouse) and large-scale relaxation mechanisms of the molecular orientation. It was found that the average relaxation time for segmental orientation is shorter and more temperature dependent than the average relaxation time for the chain extension. The segmental orientation relaxes almost totally at 170 °C ( $T_g = 148$  °C) before the chain extension even starts to relax.

## 1. Introduction

It is well known that the development of molecular orientation in amorphous polymers depends not only on the draw ratio but also on relaxation processes. This means that the total stress–strain–temperature–time history is important. A more complete understanding of the relaxation process is of great importance from both the theoretical and practical point of view.

According to Heymans,<sup>1</sup> all reasonably successful descriptions of the deformation behavior in polymers require at least two components of strain. She considers that the Brown–Windel model,<sup>2</sup> in which the deformation is divided into a segment orientation part and a chain extension part, is currently the most convincing model of orientation.

The deformation conditions necessary for obtaining high segmental orientation are in contrast to those which lead to a high chain extension. Thus, high levels of segmental orientation are achieved by rapid stretching at temperatures close to  $T_g$ , but this, on the other hand, results in low chain extension. The largest chain extension is reached at high temperatures by slow stretching, i.e., under conditions in which little segmental orientation occurs.

The relaxation of segmental orientation *during* stretching above  $T_g$  has been analyzed<sup>3,4</sup> using the Doi–Edwards model<sup>5</sup> for polymer dynamics. It was found that both the temperature dependence and the strain rate dependence of the relaxation follow the time–temperature superposition principle,<sup>3,4,6</sup> with the shift factor given by the WLF equation, and that the orientation relaxation in this respect is similar to mechanical relaxation.<sup>6,7</sup> Tassin et al.<sup>3,4</sup> have found that the relaxation of the molecular orientation obtained during constant strain rate and measured at a given draw ratio is very close to the relaxation following a step strain deformation of the same amplitude, as long as the two types of experiments are related by  $t = \dot{\epsilon}^{-1}$ , where  $t$  is the stretching time and  $\dot{\epsilon}$  is the strain rate. They nevertheless noticed that the constant strain rate deformation is more sensitive to relaxation processes at earlier stages than the step deformation.

The relaxation of segmental orientation *after* stretching above  $T_g$  has also been studied,<sup>8,9</sup> and it was found

that the results supported the reptation model for polymer melts.

The aim of this study has been to investigate for polycarbonate the relaxation of the total molecular orientation in terms of its segmental orientation and chain extension components, after step strain deformation at temperatures above  $T_g$ .

## 2. Experimental Section

**2.1. Material.** The polycarbonate (PC) used in this study was Makrolon 1143 from Bayer AG with a weight-average molecular weight of  $\bar{M}_w = 35000$ – $37000$  and a glass transition temperature of  $T_g = 148$  °C, according to the manufacturer. The polycarbonate was supplied in extruded rods with a diameter of 6 mm. Rods were chosen instead of sheets because of their better orientation homogeneity and more clearly defined stress/strain distribution under uniaxial tensile load.

**2.2. Orientation and Relaxation.** The orientation was obtained by stretching the samples at constant load to a preadjusted draw ratio. After this, the samples were kept in the stretched state, in the oven, for different times to relax and were then quenched in a water bath.

Both the stretching and the following relaxation were made in consecutive steps at constant temperature to avoid disturbances from cooling and reheating.

Three temperatures above  $T_g$  were chosen, 153, 160, and 170 °C, and two tensile loads, 84.6 and 57.4 N, which resulted in initial stresses in the samples of about 3.0 and 2.0 MPa, respectively. The highest load was chosen to produce a sufficiently high deformation rate without damaging the sample. The “nominal” draw ratio was kept constant at  $\lambda = 1.75$  but, due to small variations in local extension  $\lambda$  along the rod, where the ends had a lower  $\lambda$ , the draw ratio in the middle zone used for the measurements was somewhat higher than the nominal draw ratio. The draw ratio of 1.75 was chosen below the value of  $\lambda$  for maximum network extension calculated by Dettenmaier<sup>10</sup> to be 2.0 for PC.

Stretching under a dead load to a constant final draw ratio results in a constant maximum stress at the end of the deformation while the deformation rate is controlled by the mobility of the chains (stiffness of the sample). Thus, the procedure has the disadvantages that both strain rate and stress vary during the stretching. The advantages of the method are that it is possible to attain a high strain rate and that it is easy to quench the samples.

The samples were dried for about 12 h at 120 °C and kept at 75 °C until the moment of orientation. The rods were fixed in the orientation device (Figure 1) and placed in an oven at constant temperature. After 20 min, when the sample had reached temperature equilibrium, the sample was stretched

\* To whom correspondence should be addressed.

<sup>®</sup> Abstract published in *Advance ACS Abstracts*, August 1, 1996.

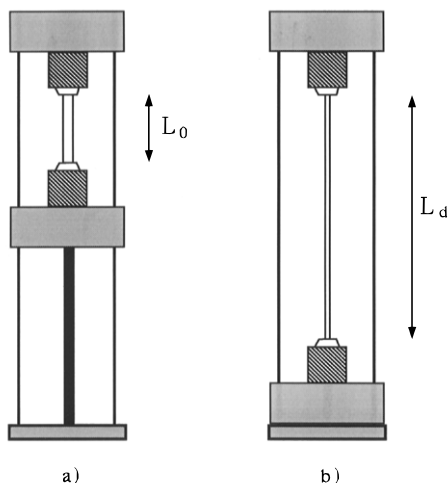


**Figure 1.** Orientation and relaxation device: (a) the unstretched sample; (b) the stretched sample.

**Table 1. Deformation Conditions**

temp (°C)	load (N)	stretching time (s)
153	84.6	11.8 ± 2.6
160	57.4	4.1 ± 0.4
160	84.6	≈0.5
170	84.6	≈0.3

by a dead load to the predetermined draw ratio. The different deformation conditions are listed in Table 1. Due to the very high deformation rate, the time to reach full extension was difficult to measure at 170 °C.

The draw ratio was defined as the ratio of the sample cross-section area before,  $A_0$ , to that after stretching,  $A_d$ :

$$\lambda_{\text{draw}} = A_0/A_d = \lambda_{dL} \quad (1)$$

This ratio is the same as the draw ratio defined as  $\lambda_{dL} = L_d/L_0$ , provided the volume is constant during the deformation. This is a reasonable assumption at the chosen temperature and deformation rate and was also checked by measuring  $\lambda_{dL}$ . The deformation was fully recoverable at all temperatures as determined by heat shrinkage measurements (see section 2.4).

To reduce possible residual thermal stresses<sup>11</sup> before microtoming, the samples were annealed at 120 °C for 24 h.

**2.3. Measurement of Segmental Orientation.** The segmental orientation was measured by infrared dichroism on a Perkin-Elmer FTIR spectrometer 1725X with a KRS-5 polarizer. To cut sections suitable for the FTIR, 3.5 mm almost cubic pieces were taken out from the oriented rods. In order to increase the contact area in the microtome sample holder, the pieces were glued with a two-component epoxy adhesive to wooden bars. In accordance with the results of earlier investigations<sup>12</sup> on the influence of the microtome cutting on the orientation of both PC and PP, the PC samples were cut at 90° to the orientation direction to ensure that the orientation was affected as little as possible by the cutting. The sections were 30 μm thick.

The dichroism,  $R$ , of the 1364 cm<sup>-1</sup> band, assigned to the inphase symmetrical bending vibration of the two methyl groups in the chain,<sup>13</sup> was calculated according to the baseline procedure presented by Lunn and Yannas.<sup>13</sup> The segmental orientation was then calculated using the Hermans orientation function,  $f$ .<sup>14</sup>

$$f = \frac{3\langle \cos^2 \theta \rangle - 1}{2} = \frac{(R_0 + 2)(R - 1)}{(R_0 - 1)(R + 2)} \quad (2)$$

where  $R_0$  is the dichroic ratio for the perfectly oriented material. If the transition moment vector  $\alpha$  is known,  $R_0$  can be calculated, since  $R_0 = 2 \cot^2 \alpha$ . For the 1364 cm<sup>-1</sup> band, this vector is perpendicular to the chain axis ( $\alpha = 90^\circ$ ).

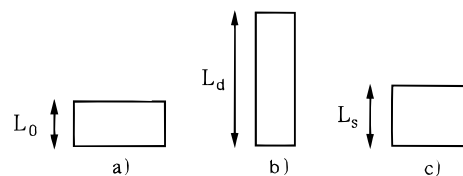


**Figure 2.** Schematic representation of the changes in sample length on deformation and shrinkage: (a) the undeformed sample; (b) the deformed sample; (c) the shrunk sample.

The accuracy of the orientation measurements is dependent on the "measuring area" and on the number of scans. In this study, the area was 7 mm<sup>2</sup> and the number of scans was 100, resulting in a standard deviation in the absorbance,  $A$ , of 0.0004 for an absorbance of 0.3 and thus a maximum deviation in the measured orientation of ±2% at a level of  $f \approx 0.08$ .

Due to the low heat transfer in polymers, the molecular orientation is usually slightly lower in the interior regions of the samples where the cooling is slower. Therefore, only sections cut between 100 and 600 μm from the surface were considered in the results.

**2.4. Measurement of Chain Extension.** If an oriented amorphous polymer is heated to a temperature above its  $T_g$ , the orientation relaxes, yielding a sample with a different shape and an isotropic state. Shrinkage tests provide a general evaluation of chain extension in flexible chain systems.<sup>15</sup> The method is simple and rapid. Figure 2 shows a schematic representation of the changes in sample length on deformation and shrinkage.

In the present case, there are two possible reasons why the sample should not shrink back to its original length: (a) The chains have slipped past each other during the deformation. (b) The chain extension has been reduced during a relaxation period with the ends of the sample clamped.

To avoid errors in the shrinkage measurements, it is important that the experiment is designed properly so that the shrinkage is fully elastic with no viscous dissipation through network slip.<sup>15</sup> The samples must therefore be thin to minimize self-constraint during shrinkage resulting from the generally poor heat transfer through polymers, and the heating must be rapid. Therefore the shrinkage measurements in this study were made on the thin microtomed slices used for the IR dichroism measurements and the heating was done in a silicone oil bath at 170 °C for 30 min. Since the samples with shortest relaxation times shrunk back to the original length ( $\lambda_{\text{draw}} = \text{CE}$ ), it indicates a properly designed measurement.

The data can be presented in different ways. As a measure of the chain extension (CE) of a sample prior to shrinkage, we have chosen

$$\text{CE} = L_d/L_s \quad (3)$$

### 3. Results

#### 3.1. Relaxation of the Segmental Orientation.

The relaxation of the segmental orientation seems to be logarithmically related to the time for relaxation,  $t$ , as shown in Figure 3. The segmental orientation immediately after deformation increases with decreasing temperature although the stretching rate as received in the orientation procedure was lower due to the higher modulus of the material. As expected, the average relaxation time for the segmental relaxation decreases with increasing temperature.

In Figure 4, the relaxation of the segmental orientation is compared for two samples oriented at different constant loads and relaxed at 160 °C. The sample stretched at higher constant load shows a higher segmental orientation, although the average relaxation time seems to have been unaffected.

**3.2. Relaxation of the Chain Extension.** The relaxation of the chain extension (Figure 5) for the

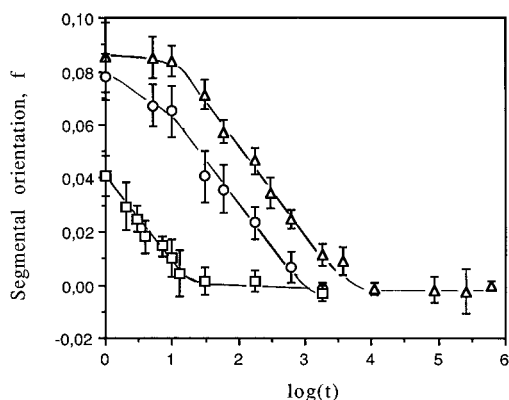


**Figure 3.** Relaxation of segmental orientation as a function of time (s) for the different orientation/relaxation temperatures: 153 ( $\Delta$ ), 160 ( $\circ$ ), and 170 °C ( $\square$ ). Each data point represents the average orientation of at least eight sections of a sample. The error bars correspond to the standard deviation of these measurements. The scatter is a result of both the orientation profile in the samples and measurement errors.

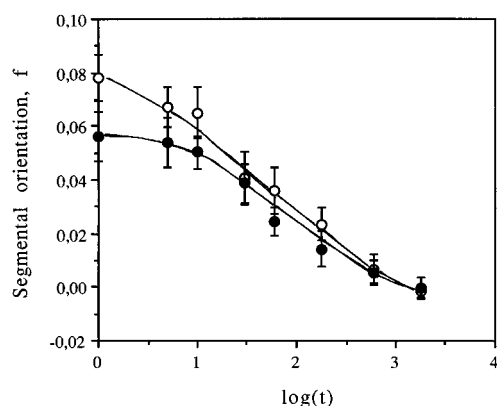


**Figure 4.** Relaxation of segmental orientation as a function of time (s) for the samples oriented and relaxed at 160 °C with dead loads of 84.6 ( $\circ$ ) and 57.4 N ( $\bullet$ ). Each data point represents the average segmental orientation of at least eight sections of a sample. The error bars correspond to the standard deviation of these measurements.

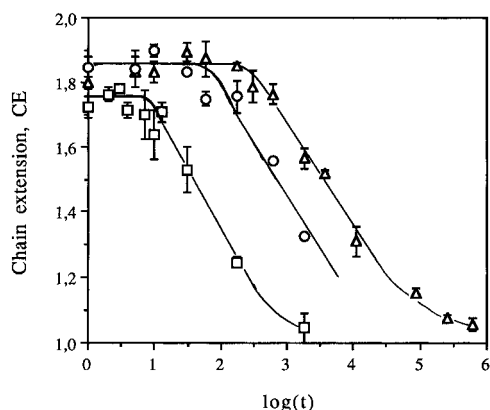


**Figure 5.** Relaxation of chain extension as a function of time (s) for samples oriented and relaxed at 153 ( $\Delta$ ), 160 ( $\circ$ ), and 170 °C ( $\square$ ). Each data point represents the average chain extension of three sections of a sample equally divided between 100 and 600  $\mu\text{m}$  from the surface. The error bars correspond to the standard deviation of these measurements.

samples stretched under the same load at different temperatures shows a clear delay time before the chain extension starts to decrease. The delay time seems to increase with decreasing temperature, indicating that the average relaxation rate decreases with decreasing

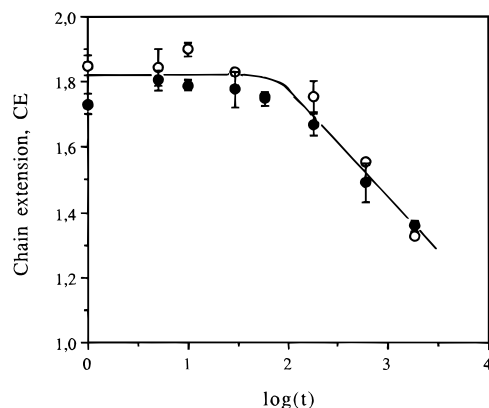


**Figure 6.** Relaxation of chain extension as a function of time (s) for samples oriented and relaxed at 160 °C with dead loads of 84.6 ( $\circ$ ) and 57.4 N ( $\bullet$ ). Each data point represents the average chain extension of three sections of a sample equally divided between 100 and 600  $\mu\text{m}$  from the surface. The error bars correspond to the standard deviation of these measurements.

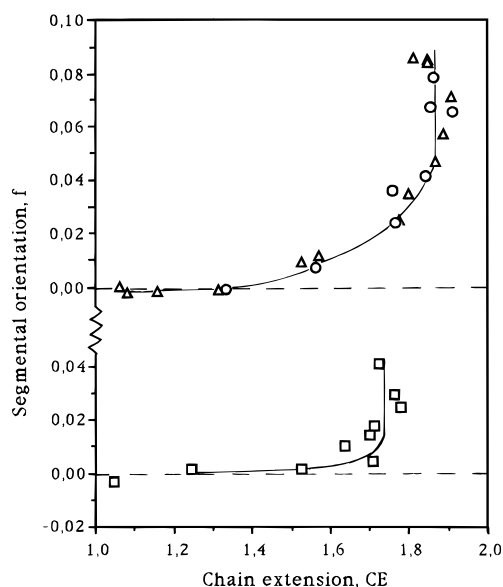


**Figure 7.** Relationship between segmental orientation and chain extension during relaxation at 153 ( $\Delta$ ), 160 ( $\circ$ ), and 170 °C ( $\square$ ).

temperature. For long relaxation times, the chain extension reaches a value of 1.0, which means that the chain extension is totally relaxed. The deformation imposed from the beginning, and kept constant during the relaxation, is however totally irrecoverable when the material is reheated above  $T_g$ . For samples stretched under different loads but at the same temperature (Figure 6), the relaxation processes seem to be unaffected, within the scatter of the data.

**3.3. Relation between the Chain Extension and the Segmental Orientation.** Figures 7 and 8 show the relation between segmental orientation and chain extension during relaxation for the different temperatures and stretching loads. As is seen in Figure 7, the curves for 153 and 160 °C coincide and the samples relaxed at 170 °C lose almost all their segmental orientation before the chain extension starts to decrease.

Figure 8 compares the relaxation at 160 °C for different dead loads. The two curves coincide. Thus the samples deformed under higher dead loads lose more segmental orientation during the time before the chain extension starts to relax.

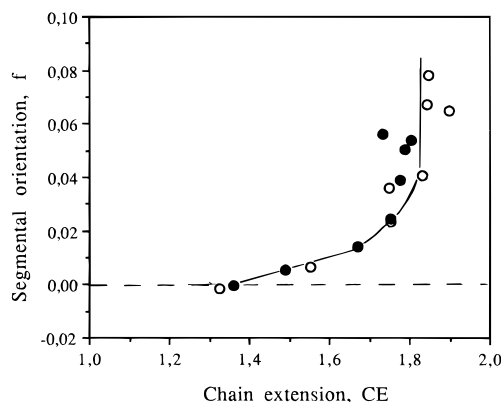


**Figure 8.** Relationship between segmental orientation and chain extension during relaxation at 160 °C with dead loads of 84.6 (○) and 57.4 N (●).

#### 4. Discussion

**4.1. Relaxation of Segmental Orientation and Chain Extension.** The purpose of this work has been to study the relaxation behavior for both the segmental orientation and chain extension in polycarbonate in order to create a better understanding of the related mechanisms.

To avoid problems related to the time needed for cooling and reheating, the orientation and the relaxation were made in two consecutive steps. By stretching the samples under a dead load, both high deformation rates and rapid cooling after the relaxation were achieved. The deformation of the chain network was completely recoverable under the deformation conditions used.

From the results, it is evident that the level of the segmental orientation immediately after deformation increases with decreasing temperature although the stretching rate was lower. This means that although the chain mobility determines the stretching rate, it does not lead to the same segmental orientation. This might suggest that it is the large-scale mobility which to a great extent determines the stretching rate and not the local scale mobility, which controls the segmental orientation.

The average relaxation time is substantially longer for the chain extension, and the average relaxation time for both the segmental orientation and the chain extension decreases with increasing temperature, although the time for segmental orientation is much more temperature dependent. This results in an almost complete relaxation of  $f$  at 170 °C, even before a relaxation of CE can be observed. This supports the suggestion by Lee and Wool<sup>8</sup> that it is possible that the molecule as a whole can lose most of its dichroism at higher temperatures by local rearrangement before relaxing from its tube.

Our results also agree with the Brown–Windel model,<sup>2</sup> which resolves the deformation into an orientational and an extensional component. The model is based on the observation that the orientation of cold-drawn PC, PMMA, and PS seems to be decoupled to some degree from strain. It was found that the molecular orientation was more susceptible to recovery than the overall strain, as also our results show.

It may be somewhat surprising that the segments can randomize without causing the sample to shrink, at least when PC is drawn as much as to 1.75 when the maximum draw ratio is 2. This point has been discussed by Dettenmaier.<sup>10</sup> This may be explained

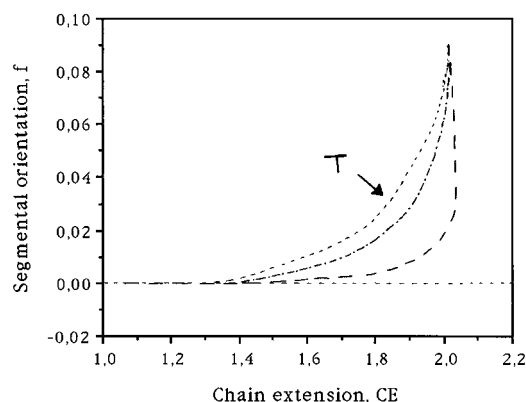


**Figure 9.** Apparent influence of temperature on the relationship between segmental orientation and chain extension.

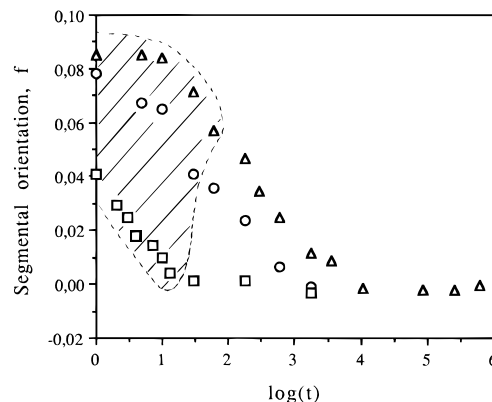


**Figure 10.** Region of Rouse relaxation for the segmental orientation relaxed at 153 (Δ), 160 (○), and 170 °C (□). Time unit: second.

by the way this limit of extensibility of the entanglement network is estimated. The limit is calculated using the entanglement molecular weight ( $M_e$ ) measured for unoriented PC. However, there is much evidence that the entanglement network (in polymer melts) is modified increasingly with the magnitude of deformation.<sup>10</sup>

As can be seen in Figure 7, the difference in temperature dependence between the average relaxation times of the segmental orientation and chain extension is too small to be observed in the temperature interval 153–160 °C, while the temperature dependence of the two processes deviate between 160 and 170 °C, causing the curves to separate. A possible theoretical diagram is drawn in Figure 9 for the temperature dependence of the relationship between  $f$  and CE. The diagram is based on the results in Figures 4 and 6, which show that the relaxation in the short-time region increases with increasing segment orientation and that the time before the chain extension starts to relax is independent of  $f$  at constant temperature.

Based on the noticed correlations between  $f$  and CE, the nature of the corresponding relaxation processes can be suggested. In the interval where chain extension remains constant although the segmental orientation decreases, the relaxation mechanism must be local. A possible mechanism is presented by the first relaxation motion of the Doi–Edwards model,<sup>5</sup> which corresponds to a Rouse relaxation within the chain between two entanglements. This process is essentially local and its kinetics, therefore, independent of the location of the segments along the chain. Figure 10 shows the corresponding region estimated from the time interval within

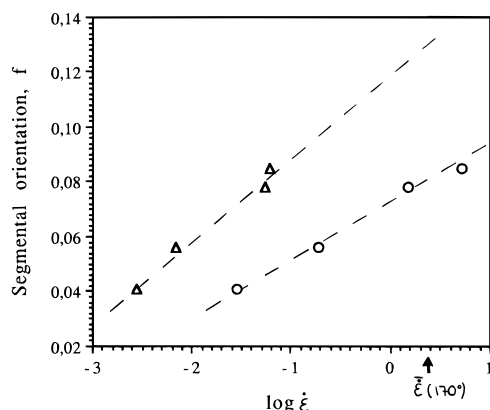


**Figure 11.** Segmental orientation shifted according to WLF for 153 ( $\Delta$ ) and 160 °C ( $\circ$ ). Time unit: second.

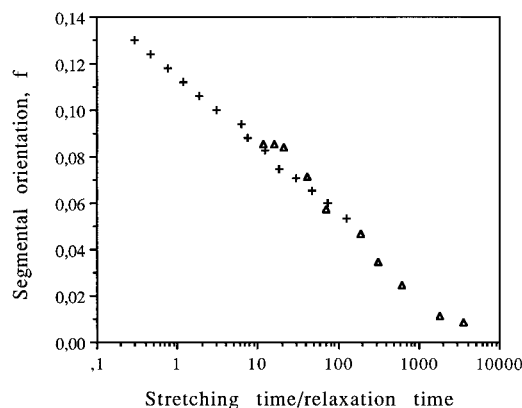


**Figure 12.** Calculated segmental orientation (+) from the time-temperature superposition principle compared with the segmental orientation after different relaxation times at 153 °C ( $\Delta$ ). Time unit: second.

which the chain extension stays constant. The relaxation of the chain extension requires large-scale motions. The Doi-Edwards model<sup>5</sup> proposes that the relaxation mechanisms for motions large enough to be hindered by surrounding chains corresponds to a contraction inside the tube and to reptation. These mechanisms overrule the Rouse mechanism.

**4.2. Relaxation during Stretching.** An interesting question is to what extent the segmental orientation relaxes during stretching. Tassin et al.<sup>3,4</sup> have found that the segmental orientation obeys the time-temperature superposition principle.

Using the WLF equation, the shift factor  $a_T$  has been calculated with the parameters  $C_1 = 11.3$  and  $C_2 = 48$  obtained from dielectrical measurements.<sup>16</sup> The average strain rate during the stretching was then transformed to the other temperatures (Figure 11). The upper limit for these curves is set by a segmental orientation corresponding to the natural draw ratio in the glassy state because increasing the strain rate transforms the polymer into the glassy state.

The calculations make it possible to estimate the segmental orientation for the same strain rate as for the 170 °C samples, marked in Figure 11. In this figure, it is also possible to read the segmental orientation resulting from different stretching times. These calculated data are compared with the segmental orientation after different relaxation times, where the stretching time has been added to the relaxation time, shown for 153 °C in Figure 12 and for 160 °C in Figure 13. The data at both temperatures correspond very well.

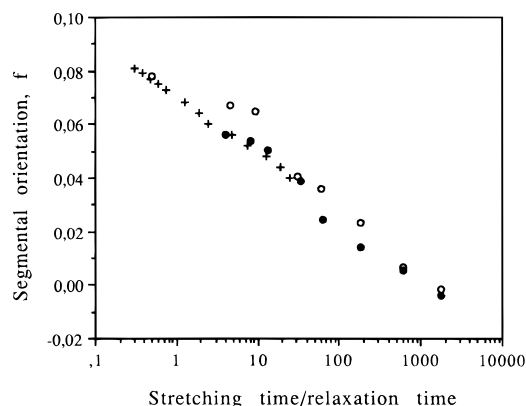


**Figure 13.** Calculated segmental orientation (+) from the time-temperature superposition principle compared with the segmental orientation after different relaxation times at 160 °C: ( $\circ$ ) stretched under the 84.6 N load; ( $\bullet$ ) stretched under the 57.4 N load. Time unit: second.

These results confirm the statement by Tassin and Monnerie<sup>3,4</sup> that it is possible to relate the relaxation of orientation in constant strain rate experiments, measured at a given draw ratio, to the relaxation following a step strain deformation of the same amplitude, as long as the two types of experiments are related by  $t = \dot{\epsilon}^{-1}$ .

## 5. Conclusions

The measurement of both segmental orientation and chain extension during relaxation makes it possible to distinguish between the local relaxation mechanism (Rouse) and the large-scale relaxation mechanisms (retraction inside the tube and reptation). The following have been found:

1. The average relaxation time for the chain extension is considerably longer than that for the segmental orientation relaxation, but less temperature dependent.
2. In certain temperature intervals, an almost total relaxation of the segmental orientation can take place without any relaxation of the chain extension.
3. At 153 and 160 °C, the segmental orientation data correspond very well with the calculated data for the segmental orientation as a function of time used to orient the sample if this time is added to the relaxation time. This result confirms the statement by Tassin and Monnerie<sup>3,4</sup> that it is possible to relate the relaxation of orientation in constant strain rate experiments, measured at a given draw ratio, with the relaxation following a step strain deformation of the same amplitude, as long as the two types of experiments are related by  $t = \dot{\epsilon}^{-1}$ .

**Acknowledgment.** The authors gratefully acknowledge the financial support given by the Swedish National Board for Industrial and Technical Development.

## References and Notes

- (1) Heymans, N. *Polymer* **1987**, *28*, 2009.
- (2) Brown, D. J.; Windel, A. H. *J. Mater. Sci.* **1984**, *19*, 1997-2056.
- (3) Tassin, J. F.; Monnerie, L. *Macromolecules* **1988**, *21*, 1846.
- (4) Tassin, J. F.; Monnerie, L.; Fetters, L. J. *Macromolecules* **1988**, *21*, 2404.
- (5) Doi, M.; Edwards, S. F. *The Theory of Polymer Dynamics*; Oxford University Press: New York, 1986.
- (6) Lefebvre, D.; Jasse, B.; Monnerie, L. *Polymer* **1983**, *24*, 1240.

- (7) Zhao, Y.; Jasse, B.; Monnerie, L. *Makromol. Chem., Macromol. Symp.* **1986**, 5, 87.
- (8) Lee, A.; Wool, R. P. *Macromolecules* **1986**, 19, 1063.
- (9) Lee, A.; Wool, R. P. *Macromolecules* **1987**, 20, 1924.
- (10) Dettenmaier, M. *Adv. Polym. Sci.* **1983**, 52/53, 57.
- (11) Saffell, J. R.; Windle, A. H. *J. Appl. Polym. Sci.* **1980**, 25, 1117.
- (12) Lundberg, L.; Sjönell, Y.; Stenberg, B.; Terselius, B.; Jansson, J. F. *Polym. Testing* **1994**, 13, 441.
- (13) Lunn, A. C.; Yannas, I. V. *J. Polym. Sci., Polym. Phys. Ed.* **1972**, 10, 2189.
- (14) Ward, I. M. *Structure and Properties of Oriented Polymers*; Applied Science Publishers, Ltd.: London, 1975.
- (15) Porter, R. S.; Chuah, H. H.; Kanamoto, T.; Measures for Polymer Chain Extension. In *High Modulus Polymers*; Zachariades, A. E., Porter, R. S., Eds.; Marcel Dekker, Inc.: New York, 1988; Chapter 9.
- (16) O'Reilly, J. M.; Sedita, J. S. *J. Non-Cryst. Solids* **1991**, 131–133, 1140.

MA9464433